



Protective effect of vitamin C against ivermectin induced nephrotoxicity in different age groups of male wistar rats: bio-histopathological study

Shereen E. Tawfeek^{1,2}, Ayat M. Domouky¹, Reham H. Abdel-Kareem¹

¹Department of Human Anatomy & Embryology, Faculty of Medicine, Zagazig University, Zagazig, Egypt, ²Department of Anatomy, Faculty of Medicine, Jouf University, Sakaka, Saudi Arabia

Abstract: Ivermectin (Ive) has exceedingly efficient against several microorganisms including viruses; therefore, it could help as a potential treatment of COVID-19. Because of increasing consumption of ivermectin and vitamin C (Vit.C) in hope to treat COVID-19, and because of ivermectin nephrotoxic effects have not been fully clarified especially in juvenile age, it was conducted to examine the histopathological and biochemical effects of ivermectin on adult and juvenile kidneys, and to assess the possible protective role of Vit.C against this potential toxicity. Rats were divided to 4 subgroups (Control subgroup, Vit.C subgroup, Ive subgroup, and Vit.C+Ive subgroup), 1 week after 4 doses of ivermectin (0.4 mg/kg Ive \pm 1.25 mg/kg Vit.C), blood samples obtained for assessment of kidney function test, part of kidneys prepared for determination of matrix metalloproteinase-9 and antioxidant enzymes assay. Other parts prepared for histopathological and ultrastructural examination. Results showed that administration of ivermectin led to attenuation in kidney function and in activities of the antioxidant enzymes and increase in matrix metalloproteinase-9 activity. In addition, there were histological damages (shrunken glomeruli, widened urinary space, cytoplasmic vacuolation and pyknotic nuclei with epithelial exfoliation, extravasated blood, and mononuclear cell infiltration) and immunohistochemistry revealed increase in percentage of Bax proapoptotic protein expression. Also, ultrastructure examination showed alteration in cell architecture. All these changes were more obvious in juvenile group while co-administration of Vit.C led to significant protection more in adult group. In conclusion, Ivermectin should be used cautiously especially in juvenile age, and co-administration of Vit.C is highly recommended.

Key words: Ivermectin, Renal toxicity, Vitamin C, COVID-19

Received June 14, 2021; Revised July 29, 2021; Accepted August 2, 2021

Introduction

The severe acute respiratory syndrome coronavirus 2 is a single-stranded RNA virus that leads to a severe acute re-

spiratory syndrome. The virus was originally called SARS-CoV-2 identified authoritatively by WHO as COVID-19. The first known case of infection was documented in early December 2019 and consequently distributed worldwide with high morbidity and mortality [1-3]. This novel virus has paralyzed not only the world's health care system but also the political and economic systems [3, 4]. Although a few medications have received emergency use authorization for COVID-19 treatment, no proven treatment has been discovered until now. A recent *in vitro* study showed that ivermectin was effective versus COVID-19 infected cell lines [5].

Corresponding author:

Reham H. Abdel-Kareem 
Department of Human Anatomy & Embryology, Faculty of Medicine,
Zagazig University, Zagazig 44511, Egypt
E-mail: reham.helmys@gmail.com

Copyright © 2021. Anatomy & Cell Biology

This is an Open Access article distributed under the terms of the Creative Commons Attribution Non-Commercial License (<http://creativecommons.org/licenses/by-nc/4.0/>) which permits unrestricted non-commercial use, distribution, and reproduction in any medium, provided the original work is properly cited.

Ivermectin offers many potential effects to treat a range of diseases, with its antimicrobial, antiviral, and anti-cancer properties as a marvel drug. It is exceedingly efficient against several microorganisms including some viruses; therefore it could help as a prospective candidate in the treatment of a broad range of viruses including COVID-19 alongside other types of single-stranded RNA viruses [6]. It interferes with nerve and muscle function of helminths and insects by binding to their glutamate-gated chloride channels driving them to open, increasing chloride ions flow, hyper-polarizing the cell membranes, paralyzing the affected tissue and finally killing them. In mammals (including humans) these channels are present only in brain and spinal cord and not affected by Iver because it cannot cross the blood brain barrier [7].

Added to having antiparasitic and antiviral effects, ivermectin triggers immunomodulation in the host, inhibiting the proliferation of cancer cells, and regulating glucose and cholesterol, some of these effects may be secondary to toxic effects on cells [8]. Recent studies demonstrated that ivermectin has antiviral action against the SARS-CoV-2 clinical isolate *in vitro*, with a single dose able to control viral replication within 24–48 hours in our system [5]. This is likely through inhibiting IMP α / β 1-mediated nuclear import of viral proteins for other RNA viruses, confirmation of this mechanism in the case of SARS-CoV-2, and if given to patients early in infection, could help to limit the viral load, prevent severe disease progression and limit person to person transmission [9]. Moreover, Shoumann et al. [10], reported that ivermectin is suggested to be a promising, effective and safe chemoprophylactic drug in management of COVID-19.

With increasing extensive demand to fight COVID-19, it is important to search about ivermectin toxic effect on several body organs. Ivermectin can enter the body orally and reach the blood and organs as the liver and kidney for metabolism. Even though it has been established as a safe and nontoxic medication for mammals [11], considering that it is a xenobiotic for the body, it probably has some effects on the oxidative stress system of the mammalian. Since xenobiotic is unknown to the host, it is expected to cause adverse effects such as toxicity, allergic response, and cancer [12]. Moreover, ivermectin has stimulated oxidative stress in the tissue of North African catfish [13]. Common adverse effects of ivermectin such as headache, pruritus, muscle pain, cough, dyspnea, nausea, vomiting, diarrhea, blurred vision, postural hypotension, and confusion were reported by clinical trials

[14, 15]. Also, it may cause nephropathy [16], psychiatric disorders [17], hepatic disorders [18], and multiorgan dysfunction syndrome [19].

Several studies showed that antioxidant substances guard cells against harmful effects of several environmental agents [20]. Vitamins, as antioxidants may preserve cells membrane function including ion transport and membrane flexibility, they may also prevent the release of Fe²⁺ and Mg²⁺ from their binding protein possibly decrease the rate of lipid peroxidation [21]. Ascorbic acid (AA) “vitamin C” is an important adjunctive therapy for respiratory infection, sepsis and COVID-19 [22]. It is a highly water soluble and acts as an efficient reducing agent [23, 24]. Vitamin C is hydrophilic and a most significant free radical scavenger in extracellular fluids, trapping radicals in the aqueous phase, and protecting bio-membranes from oxidative injury [25]. While most mammals are capable of synthesizing vitamin C in their liver or kidneys, the majority of primates (including humans), guinea pigs and some Birds and fish cannot synthesize it and must draw it from their diet. This is due to a genetic mutation that occurred 40 million years ago, blocking the transformation of glucose into AA [26].

Based on over-increasing consumption of ivermectin and vitamin C in hope to treat COVID-19 with emerging of questions about safety of its use in contact or infected children, and because of ivermectin nephrotoxic effects have not been fully clarified especially in juvenile age, this present study was conducted to examine the histopathological and biochemical effects of ivermectin on both adult and juvenile kidneys in male wistar rats, and to assess the possible protective role of vitamin C against this potential toxicity.

Materials and Methods

Chemicals

Ivermectin

Ivermectin (22,23-dihydroavermectin B) was purchased from Unipharma Egypt Company, El Obour City, Egypt as tablets each tab-6 mg. Suspension of ivermectin was dissolved in saline to make 0.2 solution.

Vitamin C

Vitamin C was purchased from Chemical Industries Development (CID) Company, Al-Harm, Giza, Egypt as tablets, each tab-500 mg was dissolved in water to make solution.

Animals

Eighty animals from 2 age groups (newborn and adults) were used in this study 40 rats each. Each group was divided randomly to 4 subgroups 10 rats each. They were obtained from the animal house, Faculty of Medicine, Zagazig University. The rats were housed in separate cages (2 rats per each cage) and maintained under standard laboratory and environmental conditions with standard rat chow. All animal experiments were carried out in accordance with relevant guidelines and regulations of the Institutional Animal Care and Use Committee, Zagazig University (ZU-IACUC committee), approval number ZU-IACUC/3/F/84/2020.

Experiment protocol

The animal groups classified as following: juvenile group (40 newborn male rats aged 2 days weighted 9–12 g) and adult group (40 adult rats aged 3 months and weighted 220–250 g) each group was randomly divided to 4 subgroups: control subgroup of each group was received 0.5 cm physiological saline, Vit.C subgroup of each group received 1.25 mg/kg vitamin C [27], Ive subgroup of each group received 0.4 mg/kg ivermectin [28] and Vit.C+Ive subgroup of each group: received 0.4 mg/kg ivermectin in concomitant with 1.25 mg/kg vitamin C. The treatments were given orally once a week for four consecutive weeks to the animals in all subgroups using gastric intubations.

One week after the last dose of ivermectin (the newborn rats become juvenile about one-month age weighted 70–90 g), blood samples were obtained for assessment of biochemical markers of kidney from all groups, body weight was measured before sacrifice. Moreover, the kidneys were harvested and weighted and immediately immersed and fixed in buffered formalin 10%, (relative kidney weight was calculated “kidney weight/body weight %”). After 24 hours of fixation the kidneys were further carefully dissected, excised and parts of it prepared for histopathological examinations and ultrastructural study. Other parts were dissected, washed with ice-cold saline, frozen in liquid nitrogen (170°C) and kept at –80°C for PCR and homogenate tissue analysis.

Serum markers analysis

Blood samples were collected, under complete aseptic conditions, from the rat retro-orbital venous plexus by means of micro-capillary glass tubes. Blood was allowed to coagulate at room temperature and then samples were centrifuged at 4,000 rpm for 20 minutes using a cooling

centrifuge (Sigma 3-30 k; Sigma-Aldrich, St. Louis, USA). The clear serum layer was separated and stored at –80°C biomarkers. Serum creatinine concentrations (SCr) (mg/dl), blood urea nitrogen (BUN) (mg/dl), were measured spectrophotometrically.

Homogenate oxidant/antioxidant kidney tissue analysis

Part of kidneys were separated instantly and homogenized in a phosphate buffer (pH 7.6), centrifuged at 20,000 rpm, 4°C for 2 hours to obtain a soluble salt part. Re-extraction of the pellets was carried out to get a soluble detergent part. The supernatant was collected and stored at –20°C. Protein concentrations were determined by the Bradford assay with Bovine serum albumin as standard (0.05–1.00 mg/ml) [29].

Total antioxidant capacity (TAC) of kidney homogenate was evaluated using FRAP assay. The FRAP reagent was prepared as a mixture of 5 ml of 10 mM of 2,4,6-tris (2-pyridyl)-s-triazine in 50 ml of 0.1 M acetate buffer (pH 3.6) and 5 ml of FeCl₃ (20 mM) in HCl (40 mM). Then, prepared FRAP reagent was incubated at 37°C for 15 minutes, and 200 µl of a kidney homogenate was mixed with 1.5 ml of the FRAP reagent and incubated for 15 minutes. The mixture was centrifuged at 12,000 rpm/15 min. Absorbance of the supernatant and standard sample was measured at 593 nm against blank [30].

Catalase assay (CAT) was performed according to Maehly and Chance [31]. One unit of catalase activity was defined as an absorbance change of 0.01 as units/min (U/min), superoxide dismutase assay (SOD) was performed according to Kakkar et al. [32]. Results are expressed in units/mg protein (U/mg protein), and glutathione peroxidase assay (GPx) was performed according to Mohandas et al. [33]. Enzyme activity was calculated as nmol NADPH oxidized/min/mg protein using a molar extinction coefficient of $6.22 \times 10^3 \text{ M}^{-1} \text{ cm}^{-1}$, results are expressed in nmol/mg protein.

Determination the reactive oxygen species (ROS) content in kidney tissues: ROS test kit (Beyotime, Shanghai, China) was used to determinate the ROS content in kidney homogenates. ROS formation was quantified and expressed as pmol DCF/min/mg protein.

Real-time quantitative reverse-transcription polymerase chain reaction (qRT-PCR) for MMP-9

Total RNA was extracted from kidney tissue using SV Total RNA Isolation System (Promega, Madison, WI, USA) and quantified spectrophotometrically at 260/280 nm. Residual

genomic DNA was removed by incubating RNA with Rnase-free DNase I. The total extracted RNA was reverse transcribed into complementary DNA (cDNA) using RTPCR kit (Stratagene, USA). Random hexamers (primers) for MMP-9 (GenBank accession number NM_009660.3 gene was used for reverse transcription of RNA. Using Forward primer: 50-CACAGACAGCCTTCTGCAAC-30, reverse primer: 50-CATTTCCCACAGCCTTGAAT-30 in 60°C, product size 141 bp. Relative changes in gene expression levels of samples to control were determined using the comparative (2DDCt) method [34, 35].

Histological and morphometric examination

Kidney specimens were embedded in paraffin after fixation in 10% formalin solution in normal saline. Blocks were sectioned at 4–5 microns then they were collected on glass slides, deparaffinized, and stained by Hematoxylin and Eosin for histopathological examination. Also, Periodic acid-Schiff (PAS) stain was used for the demonstration of polysaccharides content. The slides examined by the light electric microscope (LEICA ICC50 W), anatomy department, faculty of medicine, Zagazig University.

Image analysis software (ImageJ 1.36b; <http://rsbweb.nih.gov/ij>) was utilized to estimate histopathological findings by measuring the Cortex area (mm²), areas of glomerulus (μm²) and urinary space cross sectional (μm) in H&E kidney-stained sections. Quantitative data were estimated in 5 different non-overlapped fields for the same slide of each animal, in each animal 5 slides were counted and a total number of 25 fields of each group were counted [36].

Immunohistochemical examination

Immunohistochemistry paraffin-embedded kidney sections (4-mm-thick) were floated onto aminopropyl-triethoxysilane-coated slides, deparaffinized with xylene and hydrated in graded series of ethanol. Immunohistochemical staining was performed using avidin–biotin peroxidase complex. Endogenous peroxidase was quenched with 3% hydrogen peroxide: methanol (1:1) for 30 minutes at room temperature. Staining of formalin-fixed tissues requires boiling of tissue sections in 10 mM citrate buffer, pH 6.0 for 20 minutes followed by cooling at room temperature for 20 minutes. The primary antibodies (mice polyclonal anti-Bax, Santa Cruz Biotechnology, Dallas, Texas, USA) were diluted (1:1,000) and added to the slides. Sections were washed twice for 5 minutes in phosphate-buffered saline (PBS), followed by the addition of appropriate secondary antibody (biotinylated goat anti-rabbit immunoglobulin G diluted to 1:500), followed by incubation with peroxidase-conjugated streptavidin diluted to 1:3,000 in PBS for 15 minutes. The peroxidase reaction was performed using 0.02% chromogen 3,30 diaminobenzidine tetrahydrochloride. Sections were then counterstained with hematoxylin, dehydrated and mounted in Canada balsam [37]. Image analysis software (ImageJ 1.36b, <http://rsbweb.nih.gov/ij>) was utilized to estimate Bax immunoreactivity in 5 different non-overlapped fields About 100 epithelial cells for the same slide of each animal, in each animal 5 slides were counted and a total number of 25 fields of each group were counted. The percentage of Bax positivity was calculated.

Table 1. Anatomical parameters examination in different study groups

Variable	Juvenile group (n=10)				P-value	Adult group (n=10)				P-value
	Control subgroup	Vit.C subgroup	Ive subgroup	Vit.C+Ive subgroup		Control subgroup	Vit.C subgroup	Ive subgroup	Vit.C+Ive subgroup	
Body weight (g)	85.4±10.3	82.7±8.7	72.4±6.7 ^a	78.8±3.6	0.0039	243±26	233±22	201±16 ^b	225±18 ^c	0.0006
% of change		-3.1±1.3	-15.3±2.5	-7.7±1.4			-2.4±1.2	-11.3±2.8 ^c	-6.9±0.9	
Kidney weight (g)	0.58±0.06	0.59±0.05	0.45±0.04 ^a	0.52±0.1	0.0230	1.12±0.23	1.18±0.33	1.02±0.18	1.06±0.24	0.1809
% of change		+1.7±0.2	-18.4±0.5	-10.3±0.4			+5.1±0.3 ^f	-9.2±0.4 ^f	-6.6±0.4 ^f	
Kidney/body weight %	0.64±0.18	0.67±0.17	0.58±0.14	0.61±0.09	0.5735	0.46±0.12	0.47±0.16	0.44±0.09	0.45±0.21	0.9744
% of change		+4.5±0.5	-9.4±0.5	-4.7±0.3			+1.8±0.2 ^f	-3.17±0.5 ^f	-1.7±0.4 ^f	

Values are presented as mean±SD. Juvenile group: aged 2 days, weighted 9–12 g; Adult group: aged 3 months, weighted 220–250 g. Ive, ivermectin; Vit.C, vitamin C. One-way ANOVA ($P>0.05$, no significant differences; $P<0.05$, significant differences; $P<0.001$, highly significant differences). Least significant difference (LSD) test were used to show significance between different subgroups in the same group: ^asignificant vs control subgroup, ^bhighly significant vs control subgroup, ^csignificant vs Ive subgroup, ^dhighly significant vs Ive subgroup. *t*-test was used to show significance between percentage of change happened in (Ive and Vit. C+Ive subgroups) from control subgroup to corresponding subgroup in the two study groups: ^esignificant vs corresponding subgroup, ^fhighly significant vs corresponding subgroup.

Ultrastructure examinations

Kidney specimens were fixed using 2.5% glutaraldehyde for 24–48 hours, followed by washing three to four times in phosphate buffer (pH 7.2–7.4). The specimens were then post-fixed in a buffered solution of 1% osmium tetroxide for 2 hours, after that washed in a similar buffer four times for 20 minutes each. Fixed specimens were dried out in increasing concentrations of ethyl alcohol (30%, half, 70%, 90%, and 100%), cleared in two changes of propylene oxide and inserted in Epon resin. The pitch squares underwent a

process of trimming to get rid of the surplus tissue. Ultrathin sections (60–90 nm thick) and illustrative fields of semithin sections were chosen and were cut with a diamond knife using a Reichert OMVs ultra microtome, mounted on copper frameworks. These semi-thin sections were subjected to double staining with uranyl acetate and lead citrate [38]. The grids were examined and photographed using a transmission electron microscope (JEOL JEM-1010, Tokyo, Japan) at the Mycology and Regional Biotechnology Center, Al Azhar University for Boys, Cairo, Egypt.

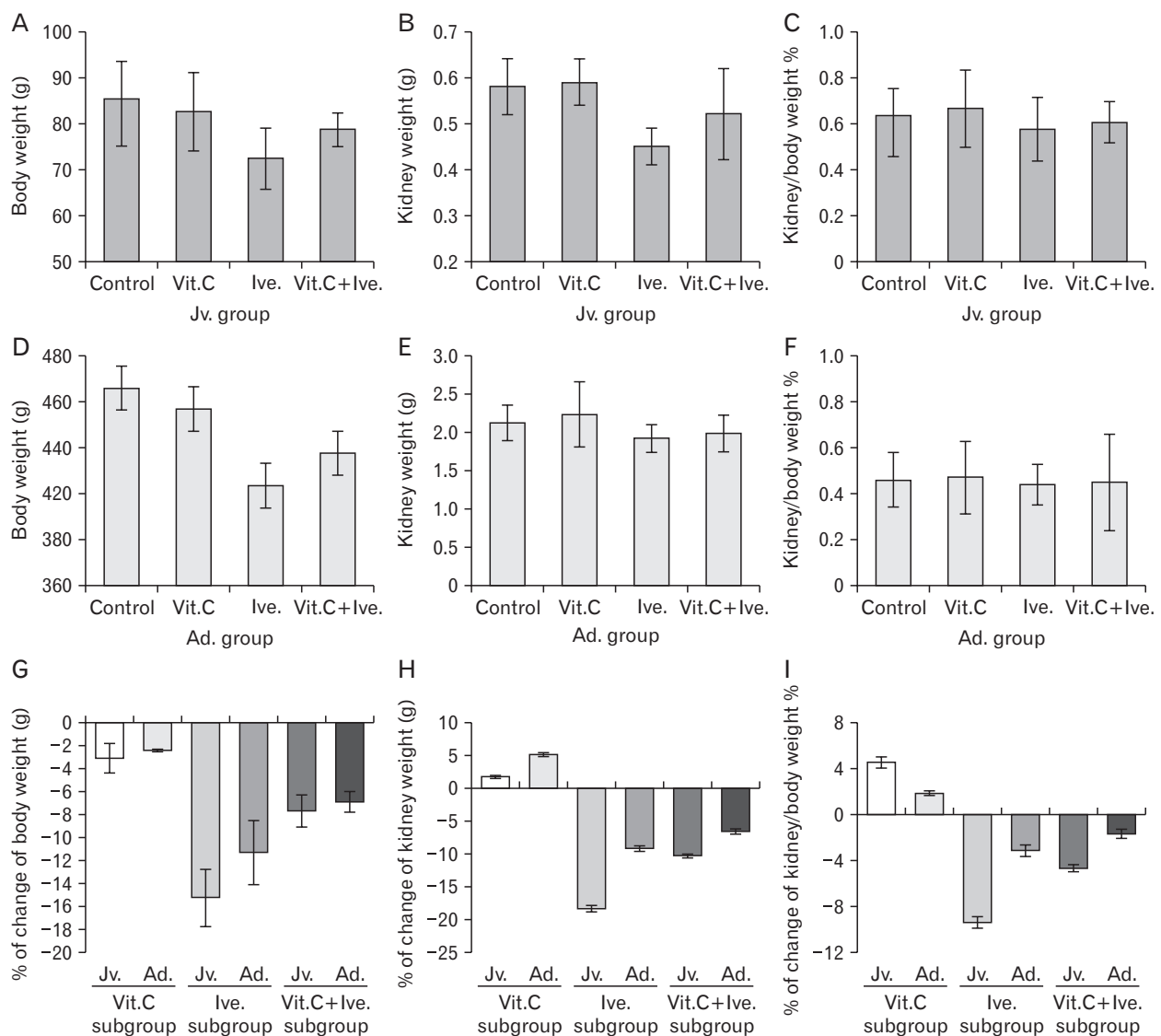


Fig. 1. Anatomical parameters examination in different study groups showing that Juvenile (Jv) rats treated with ivermectin (Ive subgroup) have a significant decrease in body weight (A) and kidney weight (B) compared with control and vitamin C (Vit.C) subgroups, while kidney weight/body weight % (C) remain insignificant difference. Adult (Ad) rats reveal significant difference in body weight (D) and no significant difference neither in kidney weight (E) nor kidney weight/body weight % (F). The percentage of change happen in corresponding Ive subgroups, the juvenile rats exhibit more body weight loss (G), also more kidney weight loss (H, I). Values are presented as mean \pm SD.

Statistical analysis

The collected biochemical and morphometric data was statistically analyzed using SPSS program (Statistical Package for Social Science) version 18.0. Descriptive statistics were given as mean±standard deviation (SD). Numbers with percentages (%) were used for nominal variables. One-way ANOVA were used to compare the mean values of different groups. Multiple comparisons were estimated by the least significant difference (LSD) test. Moreover, *t*-test was used to show significance between corresponding subgroups in the two study groups, a value of $P<0.05$ was statistically significant, a value of $P<0.001$ was highly statistically significant, and a value of $P>0.05$ was non-statistically significant.

Results

Anatomical parameters examination

Juvenile rats treated with ivermectin (Ive subgroup) showed a significant decrease in body weight and kidney weight compared with control and Vit.C subgroups, while kidney weight/body weight % remained insignificant difference. Consumption of vitamin C parallel with ivermectin in Vit.C+Ive subgroups led to partial protection from this weight loss. On the other hand, adult rats revealed significant difference in body weight and no significant difference neither in kidney weight nor kidney weight/body weight %

between all subgroups (Table 1, Fig. 1A–F).

When comparing the percentage of change happened in corresponding Ive subgroups (from the control subgroup) in the two study groups, the juvenile rats exhibited more body weight loss (-15.3 ± 2.5 vs -11.3 ± 2.8 in adult), also more kidney weight loss (-18.4 ± 0.5 vs -9.2 ± 0.4 in adult). Vitamin C supplementation in Vit.C+Ive subgroups showed protective effect in both groups, but it was relatively less in juvenile group due to more effect of ivermectin at this young age (Table 1, Fig. 1G–I).

Serum markers analysis results

Kidney function test showed that rats treated with ivermectin (Ive subgroup) had a highly significant increase in the kidney function marker; SCr, BUN, as compared to control and Vit.C subgroups. Consumption of vitamin C parallel with ivermectin in juvenile rats led to partial protection from this deterioration, while in adult rats vitamin C led to nearly full protection from this deterioration. Accordingly, comparing of both Ive, subgroups the juvenile group showed more elevated kidney function marker however vitamin C gave better protection in adult group (Table 2, Fig. 2A, B).

Homogenate kidney tissue analysis for oxidant/antioxidant activities

Measuring TAC as well as the activities of the antioxidant

Table 2. Biochemical parameters analysis in different study groups

Variable	Juvenile group (n=10)				P-value	Adult group (n=10)				P-value
	Control subgroup	Vit.C subgroup	Ive subgroup	Vit.C+Ive subgroup		Control subgroup	Vit.C subgroup	Ive subgroup	Vit.C+Ive subgroup	
Serum markers										
SCr	1.12±0.3	1.08±0.42	5.37±1.46 ^b	2.23±0.81 ^{ad}	<0.001	1.34±0.15	1.12±0.63	4.07±1.76 ^{bc}	2.11±0.34 ^{de}	<0.001
BUN	18.43±3.64	18.23±3.2	68.65±10.46 ^b	35.36±5.72 ^{bd}	<0.001	20.22±3.3	19.79±4.12	56.35±8.37 ^b	26.37±5.6 ^d	<0.001
Kidney homogenate										
TAC	82±13	95±21 ^b	45±14	75±10 ^d	<0.001	87±11	94±15 ^b	52±17	73±7 ^c	<0.001
CAT	11.6±1.5	12.2±1.7	7.8±1.1 ^b	10.2±1.6 ^c	<0.001	13.2±1.7	15.7±1.3 ^{ac}	9.7±1.1 ^{bc}	12.2±1.4 ^{adc}	<0.001
SOD	8.2±1.7	9.6±1.1	4.6±0.6 ^b	6.5±1.2 ^{ac}	<0.001	9.4±0.7	10.6±1.4	6.8±1.6 ^{bc}	8.2±0.9 ^{acc}	<0.001
GPx	20.6±2.7	25.4±2.4 ^b	12.4±1.6 ^b	18.6±2.4 ^d	<0.001	23.2±4.3	25.7±3.2	17.8±2.6 ^{af}	21.4±1.9 ^e	<0.001
ROS	3±2	2±2	15±4 ^b	7±3 ^d	<0.001	4±1	3±2	9±3 ^b	5±4 ^c	<0.001
qRT-PCR										
MMP9	0.35±0.12	0.32±0.15	2.11±0.47 ^b	0.88±0.21 ^{bd}	<0.001	0.73±0.24 ^c	0.64±0.15 ^c	3.2±0.53 ^{bc}	1.82±0.54 ^{bdc}	<0.001

Values are presented as mean±SD. Juvenile group: aged 2 days, weighted 9–12 g; Adult group: aged 3 months, weighted 220–250 g. Ive, ivermectin; Vit.C, vitamin C; SCr, serum creatinine concentrations (mg/dl); BUN, blood urea nitrogen (mg/dl); TAC, total antioxidant capacity (μmol/volume); CAT, catalase (U/min); SOD, superoxide dismutase (U/mg protein); GPx, glutathione peroxidase (nmol/mg protein); ROS, reactive oxygen species (pmol DCF/min/mg protein); qRT-PCR, real-time quantitative reverse-transcription polymerase chain reaction; MMP9, matrix metalloproteinase-9. One-way ANOVA ($P>0.05$, no significant differences; $P<0.05$, significant differences; $P<0.001$, highly significant differences). Least significant difference (LSD) test were used to show significance between different subgroups in the same group: ^asignificant vs control subgroup, ^bhighly significant vs control subgroup, ^csignificant vs Ive subgroup, ^dhighly significant vs Ive subgroup. *t*-test was used to show significance between corresponding subgroups in the two study groups: ^esignificant vs corresponding subgroup, ^fhighly significant vs corresponding subgroup.

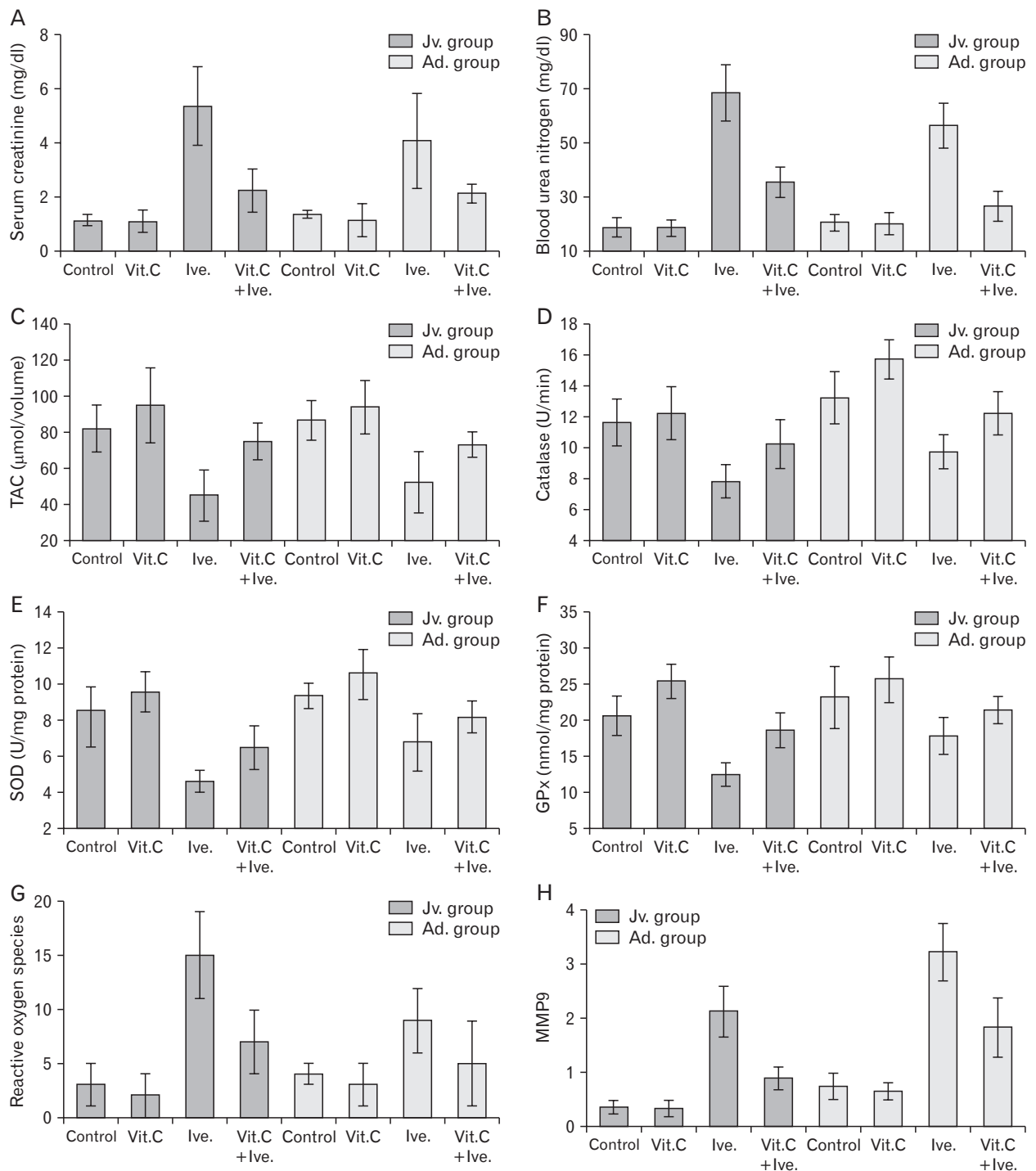


Fig. 2. Biochemical parameters analysis in different study groups showing that rats treated with ivermectin (Ive subgroup) have a highly significant increase in the kidney function marker; Serum creatinine concentrations (A), Blood urea nitrogen (B). Measuring the activities of the TAC (C), antioxidant enzymes catalase assay (CAT) (D), superoxide dismutase assay (SOD) (E), glutathione peroxidase assay (GPx) (F), and reactive oxygen species (G) showing that administration of vitamin C (Vit.C) alone leads to increase in antioxidant enzymes activities, on the other hand, rats treated with ivermectin (Ive subgroups) display a highly significant decrease in the activities of the antioxidant enzymes, comparing juvenile (Jv) and adult (Ad) groups showing that Jv rats have more decline in oxidants activity in treated group and less protected effect of Vit.C. Matrix metalloproteinase 9 (MMP9) is statistically significantly higher in Ive treated subgroups (H). Values are presented as mean±SD. TAC, total antioxidant capacity.

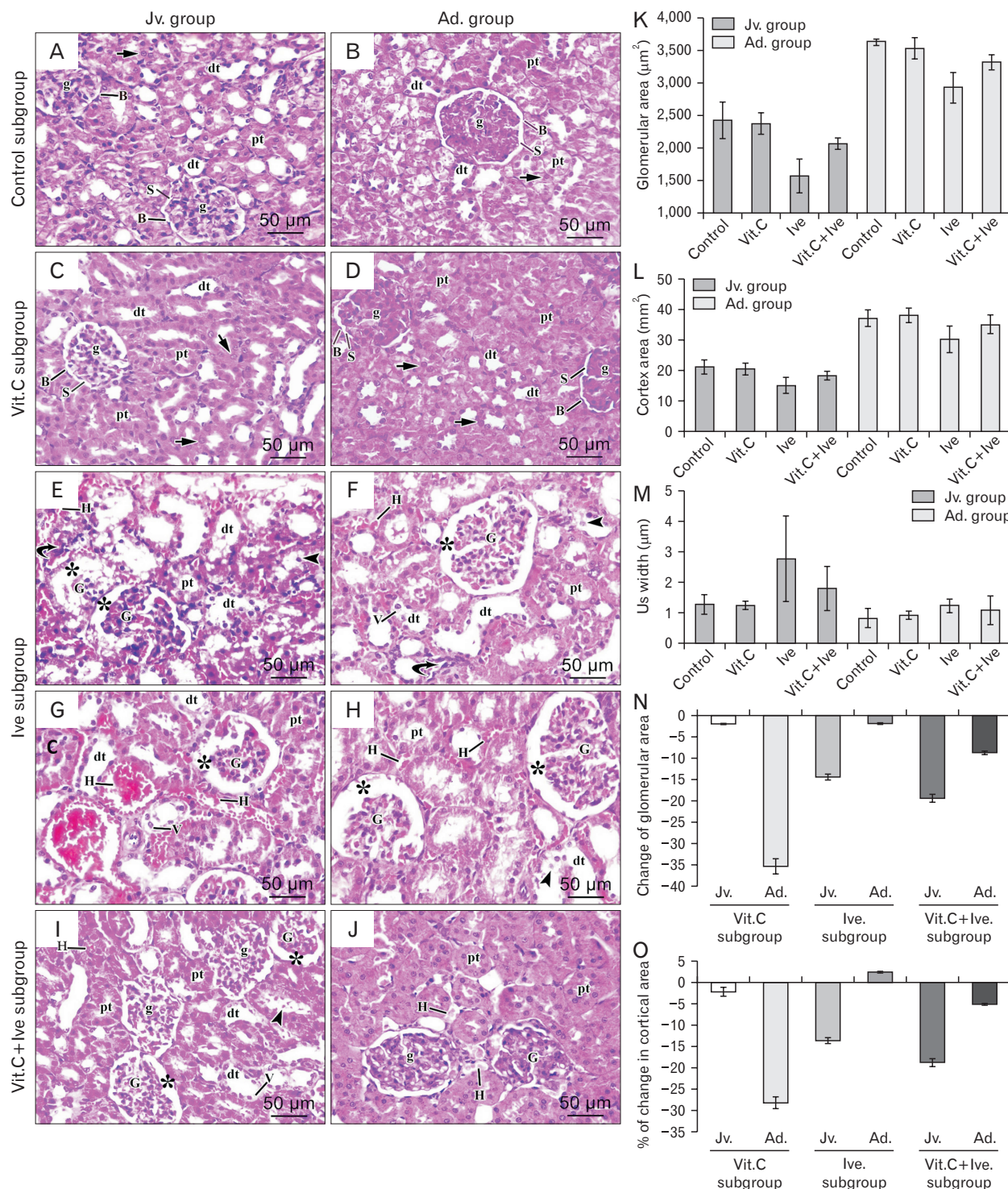


Fig. 3. H&E ($\times 400$) stained sections of renal tissues in different experimental groups: control and vitamin C (Vit.C) subgroups (A–D) showing; normal shaped glomeruli (g), normal renal space (S) lined by parietal layer of Bowman’s capsules (B) and renal tubules (dt, distal tubule; pt, proximal tubule) lined by normal cells with vesicular nuclei (short arrow). Ivermectin treated sub groups (Ive subgroup) (E–H) showing; shrunken glomeruli (G), widened urinary space (*), dilated tubules (dt & pt) lined by vacuolated cells with pyknotic nuclei (V), some desquamated cells in the lumen (arrow head), inflammatory cell infiltration (curved arrows) and extravasated blood (H). Vit.C+Ive subgroups (I, J) showing; normal shaped glomeruli (g) and tubules (dt, distal tubule; pt, proximal tubule), some shrunken glomeruli (G), relatively wide renal space (*) and some extravasated blood (H). In (I), few tubules exhibit pyknotic nuclei with cytoplasmic vacuolation (V) and epithelial cell exfoliation (arrow head). Morphometrically, in the Ive subgroups, cortical surface area (L) and glomerular area (K) showing significant decrease with significant increase in urinary space cross sectional (M), these changes are more obvious in juvenile (Jv) group (N, O) than adult (Ad) group.

enzymes CAT, SOD and GPx in the kidney tissues of different study subgroups in both juvenile and adult rats showed that administration of vitamin C alone led to increase in TAC and antioxidant enzymes activities, on the other hand, rats treated with ivermectin (Ive subgroups) displayed a highly significant decrease in the activities of the TAC, CAT, SOD, and GPx with significant increase in ROS. While consumption of vitamin C parallel with ivermectin in both Vit. C+Ive subgroups exhibited stability of oxidant/antioxidant activities near control group. Comparing juvenile and adult groups showed that juvenile rats had more decline in oxidants activity in treated group and less protected effect of vitamin C (Table 2, Fig. 2C–G).

Real-time quantitative reverse-transcription polymerase chain reaction (qRT-PCR) for MMP-9

PCR examination of samples obtained from different study subgroups had convincingly showed that matrix metalloproteinase 9 (MMP9) was statistically significantly higher in ivermectin treated subgroups compared to control which indicate basement membrane degradation as MMP9 has been regarded as one of the major enzymes responsible for basement membrane degradation. While consumption of vitamin C parallel with ivermectin exhibited partial stability against this degradation. Comparing juvenile and adult groups showed that adult rats had higher level of MMP9 in all subgroups (Table 2, Fig. 2H).

H&E Histopathological and morphometric results

H&E stained sections of control as well as Vit.C subgroups in both juvenile and adult rats showed nearly similar results

with normal renal histology; corpuscles formed of a dense rounded glomerulus surrounded by a parietal layer of Bowman's capsule with the urinary space in-between, moreover, proximal convoluted tubules were lined with low columnar cells with spherical basal nuclei and distal convoluted tubules were lined with low cuboidal cells with rounded central nuclei (Fig. 3A–D).

On other hand, sections of Ive subgroup of juvenile rats showed extensive renal damage with extremely shrunken glomeruli and a widened urinary space in-between, proximal and distal convoluted tubules were dilated, and their lining cells showed extensive cytoplasmic vacuolation with pyknotic nuclei, and also epithelial cell exfoliations were present, moreover, there were extensive extravasated blood and mononuclear cell infiltration (Fig. 3E, G). Sections of Ive subgroup of adult rats showed less extensive renal damage with shrunken glomeruli and widened urinary space, fewer areas of extravasated blood and mononuclear cell infiltration, with also some of proximal and distal convoluted tubules are dilated and their lining cells showed pyknotic nuclei with some cytoplasmic vacuolation and epithelial cell exfoliations (Fig. 3F, H).

Vit.C+Ive subgroups in both juvenile and adult rats showed improvement in the renal alterations. This improvement was more obvious in adult rats as the damage was less extensive than the juvenile ones. Some glomeruli were slightly shrunken with relatively wide renal space and there was few extravasated blood in both groups. Few tubules exhibit pyknotic nuclei with cytoplasmic vacuolation and epithelial cell exfoliation in juvenile group (Fig. 3I, J).

The histopathological alterations were confirmed mor-

Table 3. Morphometric analysis for H&E and immunohistochemical histological examination in different study groups

Variable	Juvenile group (n=10)				P-value	Adult group (n=10)				P-value
	Control subgroup	Vit.C subgroup	Ive subgroup	Vit.C subgroup		Control subgroup	Vit.C subgroup	Ive subgroup	Vit.C+Ive subgroup	
H&E										
Cortex area (mm ²)	21.11±2.3	20.45±1.9	15.15±2.7 ^b	18.21±1.5 ^{bc}	<0.001	37.21±2.7	38.12±2.4	30.21±4.3 ^b	35.12±3.1 ^d	<0.001
% of change		-2.2±0.7	-28.3±1.4	-13.7±2.3			+2.4±0.2	-18.8±1.3 ^f	-5.2±1.1 ^f	
Glomerular area (µm ²)	2,423±281	2,376±172	1,573±264 ^b	2,073±92 ^{ad}	<0.001	3,640±47	3,536±163	2,932±244 ^b	3,322±121 ^{ad}	<0.001
% of change		-1.9±0.6	-35.4±4.7	-14.4±1.4			-1.8±0.3	-19.4±2.2 ^f	-8.7±1.9 ^f	
Urinary space width (µm)	1.27±0.32	1.24±0.14	2.76±1.4 ^a	1.79±0.73 ^c	<0.001	0.82±0.32	0.91±0.14	1.23±0.22 ^b	1.08±0.47	0.0284
Immunohistochemical										
% Bax positivity	5.23±0.15	5.09±0.32	35.37±4.43 ^b	17.23±2.43 ^{bd}	<0.001	6.32±0.09	6.02±0.43	29.07±1.16 ^{bc}	9.16±1.94 ^{df}	<0.001

Values are presented as mean±SD. Juvenile group: aged 2 days, weighted 9–12 g; Adult group: aged 3 months, weighted 220–250 g. Ive, ivermectin; Vit.C, vitamin C. One-way ANOVA ($P>0.05$, no significant differences; $P<0.05$, significant differences; $P<0.001$, highly significant differences). Least significant difference (LSD) test were used to show significance between different subgroups in the same group: ^asignificant vs control subgroup, ^bhighly significant vs control subgroup, ^csignificant vs Ive subgroup, ^dhighly significant vs Ive subgroup. *t*-test was used to show significance between corresponding subgroups in the two study groups: ^esignificant vs corresponding subgroup, ^fhighly significant vs corresponding subgroup.

phometrically, in juvenile rats, there were less cortical surface area in the Ive subgroup compared with control subgroups (-28.3 ± 1.4 in juvenile rats vs -18.8 ± 1.3 in adult rats), glomerular area showed significant decrease in Ive subgroup compared with control subgroups (-35.4 ± 4.7 in juvenile rats vs -19.4 ± 2.2 in adult rats). This glomerular shrinkage accompanied by significant increase in urinary space cross

sectional. Consumption of vitamin C parallel with ivermectin led to partial protection from these histopathological changes (Table 3, Fig. 3K–O).

PAS histopathological results

PAS-stained sections of control as well as Vit.C subgroups in both juvenile and adult rats showed that, convoluted tu-

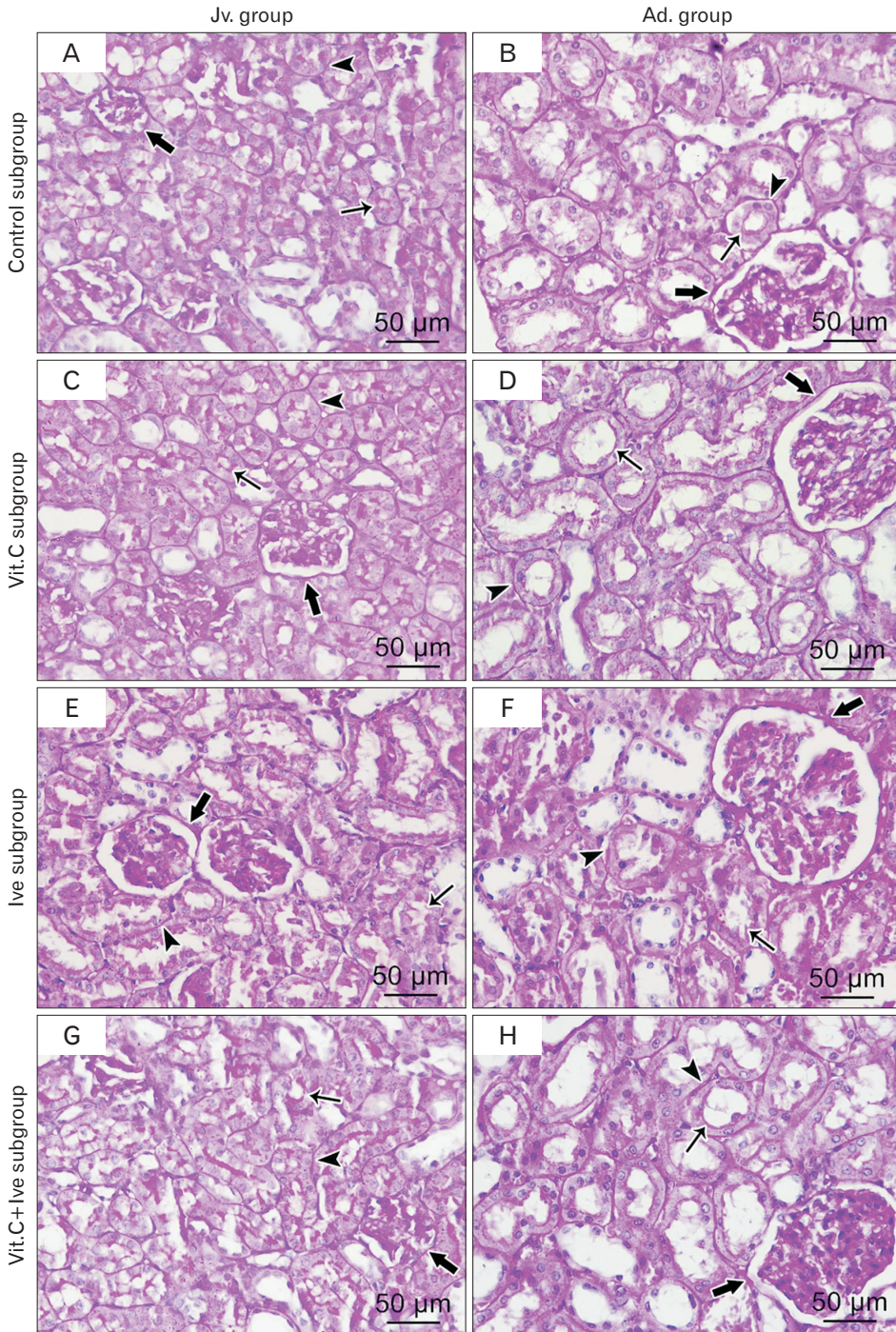


Fig. 4. PAS stained ($\times 400$) sections of renal tissues in different experimental groups (A–D) (control & Vit.C) showing; well-formed tubular basement membranes (arrow heads), Basement membranes of Bowman’s capsules appear as thin regular PAS+Ive (thick arrows) and well developed brush borders of proximal convoluted tubule (arrows). Ive treated sub groups, (E, F) showing; strong positive PAS reaction of thickened basement membrane of both Bowman’s capsule (thick arrows) and renal tubules (arrow heads) and discontinuity PAS reaction at the brush borders of proximal tubular cells (arrows). Vit.C+Ive subgroups (G, H) showing; PAS positive reaction at the thin Bowman’s capsule (thick arrows) and tubular basement membrane (arrow heads) and continued brush border of proximal tubules (arrows). Vit.C, vitamin C; Ive, ivermectin; Jv, juvenile; Ad, adult.

bules were bounded by well-formed tubular basement membranes. The proximal convoluted tubules had well developed brush borders along their lumen. Basement membranes of Bowman’s capsules appeared as thin regular PAS+Ive (Fig. 4A–D). On other hand, sections of Ive subgroups revealed strong positive PAS reaction of thickened basement membrane of both Bowman’s capsule and renal tubules. But PAS

reaction showed discontinuity at the brush borders of proximal tubular cells (Fig. 4E, F). Vit.C+Ive subgroups in both juvenile and adult rats showed improvement in the renal alterations, as PAS positive reaction at the thin Bowman’s capsule and tubular basement membrane and brush border of proximal tubules to some degree was preserved. This improvement was more obvious in adult rats as the damage was

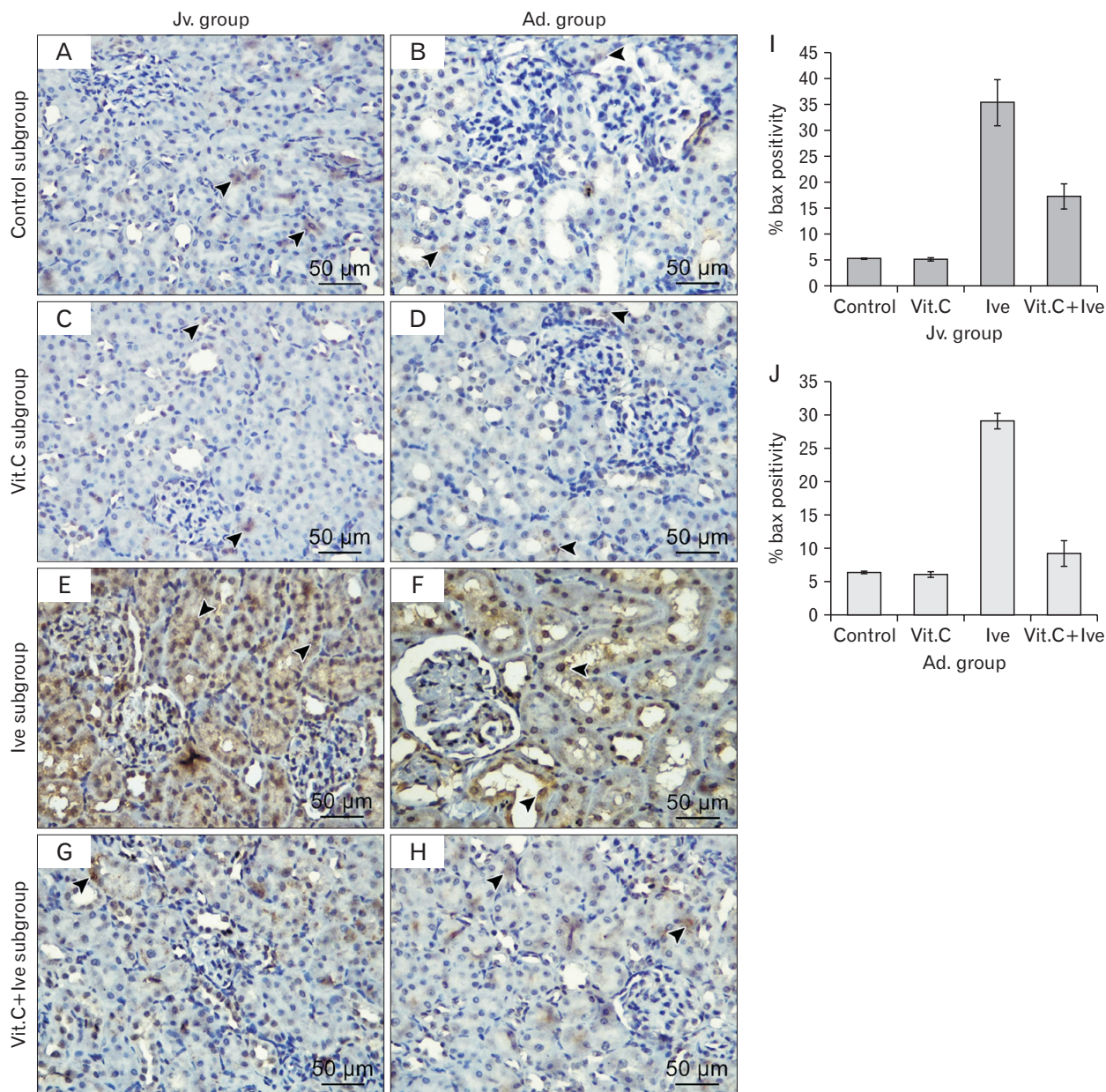


Fig. 5. Bax immune-stained (×400) sections of renal tissues in different experimental groups showing; positive proapoptotic protein in the cytoplasm of renal tubules (arrow heads) is normally expressed in control and Vit.C subgroups (A–D), while Ive treated subgroups (E, F) display patchy expression. Vit.C+Ive subgroups (G, H) showing improvement in the Bax proapoptotic protein expression. Morphometrical analysis of percentages of Bax positivity showing high significant increase in Ive subgroups and significant increase in Vit.C+Ive subgroups (I, J). Vit.C, vitamin C; Ive, ivermectin; Jv, juvenile; Ad, adult.

less extensive than the juvenile ones (Fig. 4G, H).

Bax immunohistochemistry results

Immune-stained for Bax proapoptotic protein showed normal expression in cytoplasm of tubular epithelial cells in both control and Vit.C subgroups in both juvenile and adult rats (Fig. 5A–D). Otherwise, Ive subgroups in both groups displayed patchy expression of Bax proapoptotic protein in the cytoplasm of renal tubules which was more obvious in juvenile group than in adult (Fig. 5E, F). Vit.C+Ive subgroups in both groups demonstrated a marked improvement in the Bax proapoptotic protein expression especially in adult group rats (Fig. 5G, H).

Morphometrical analysis of percentages of Bax positivity in control and Vit.C subgroups were $5.23\% \pm 0.15\%$ and $5.09\% \pm 0.32\%$ in juvenile rats and $6.32\% \pm 0.09\%$ and $6.02\% \pm 0.43\%$ in adult rats, respectively. These percentages

were highly increased in Ive subgroups ($35.37\% \pm 4.43\%$ in juvenile rats and $29.07\% \pm 1.16\%$ in adult rats), and in Vit.C+Ive subgroups were significantly increased ($17.23\% \pm 2.43\%$ in juvenile rats and $9.16\% \pm 1.94\%$ in adult rats) (Table 3, Fig. 5I, J).

Ultrastructure results

The ultrastructure examinations of control along with Vit. C subgroups in both juvenile and adult rats showed normal renal architecture. The proximal convoluted tubular cells displayed rounded heterochromatic nucleus with prominent nucleolus and intact nuclear envelop, intact apical microvilli prominent in adult group while the microvilli were less developed or absent in juvenile group, abundant parallel electron dense mitochondria were observed situated between the nucleus and uniformly thin basal cell membrane (Fig. 6A–D, G, H). In glomerular cells, besides numerous organelles,

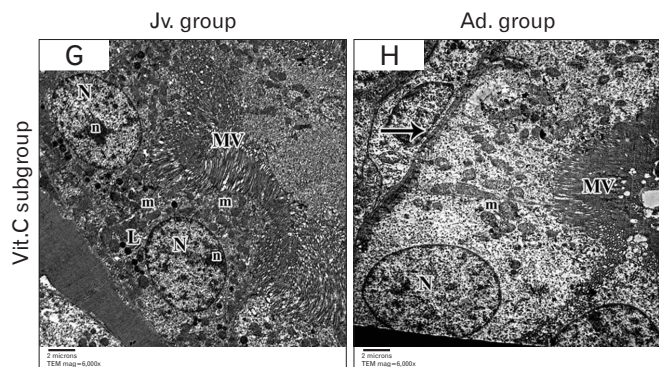
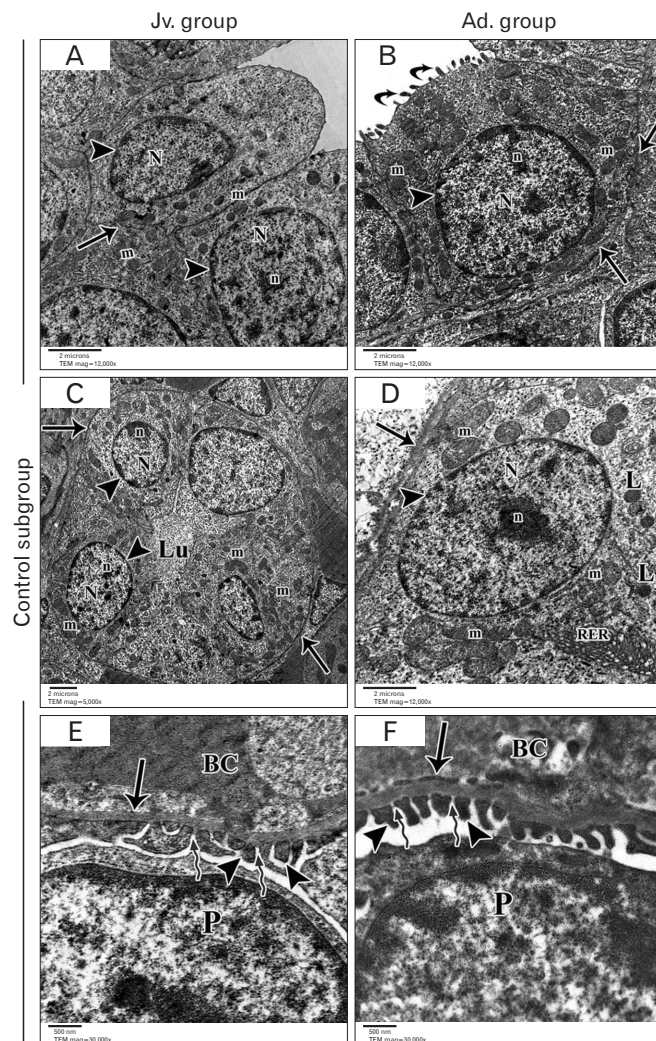


Fig. 6. Electron micrographs of kidney tubules of control subgroup; juvenile (Jv) (A: proximal tubule, $\times 12,000$; C: distal tubule, $\times 6,000$) and adult (Ad) (B: proximal tubule, $\times 12,000$; D: distal tubule, $\times 12,000$) showing the following features: N, normal nucleus; n, nucleolus; m, mitochondria; arrow head, nuclear envelop; arrow, basal lamina; curved arrow, apical microvilli; Lu, lumen; L, lysosomes; RER, rough endoplasmic reticulum and the electron micrographs of glomerulus in both Jv (E: $\times 30,000$) and Ad (F: $\times 30,000$) of the control subgroup showing; P, podocyte nucleus; BC, blood capillary; arrow, basal lamina; arrow head, foot process of podocytes; zigzag arrow, septum between foot process. Electron micrographs of proximal tubule of Vit.C subgroup of Jv (G: $\times 6,000$), and Ad (H: $\times 6,000$) showing; N, normal nucleus; n, nucleolus; m, mitochondria; L, lysosomes; MV, microvilli; arrow, basement membrane. Vit.C, vitamin C; Ive, ivermectin.

podocytes had several cytoplasmic extensions (the primary processes) which wrapped around the glomerular capillaries giving rise to numerous secondary foot processes called pedicles (Fig. 6E, F).

Nevertheless, Ive subgroups displayed severe damage of renal ultrastructure in both groups where the proximal convoluted tubular cells displayed wide areas of cytoplasmic rarefaction, extremely degenerated irregular nuclei, mitochondria appeared ballooned with damaged cristae, large secondary lysosomes, markedly thickened irregular basal cell membrane and completely degenerated microvilli with extrav-

asated blood in the lumen or intraluminal casts (Fig. 7A–D). In glomerular cells, most of the foot processes were destructed or lost or fused together (Fig. 7E, F).

Consumption of vitamin C parallel with ivermectin led to partial protection from this deterioration in adult rats as well as the juvenile ones, in adult rat there was adequate improvement of viability of the cells of convoluted tubules which exhibited normal heterochromatic nucleus, intact nuclear envelop, intact basal infoldings and relatively thick basal lamina (Fig. 7H) some cells still exhibited apoptotic shrunken nucleus (Fig. 7J). In juvenile rats there was also a

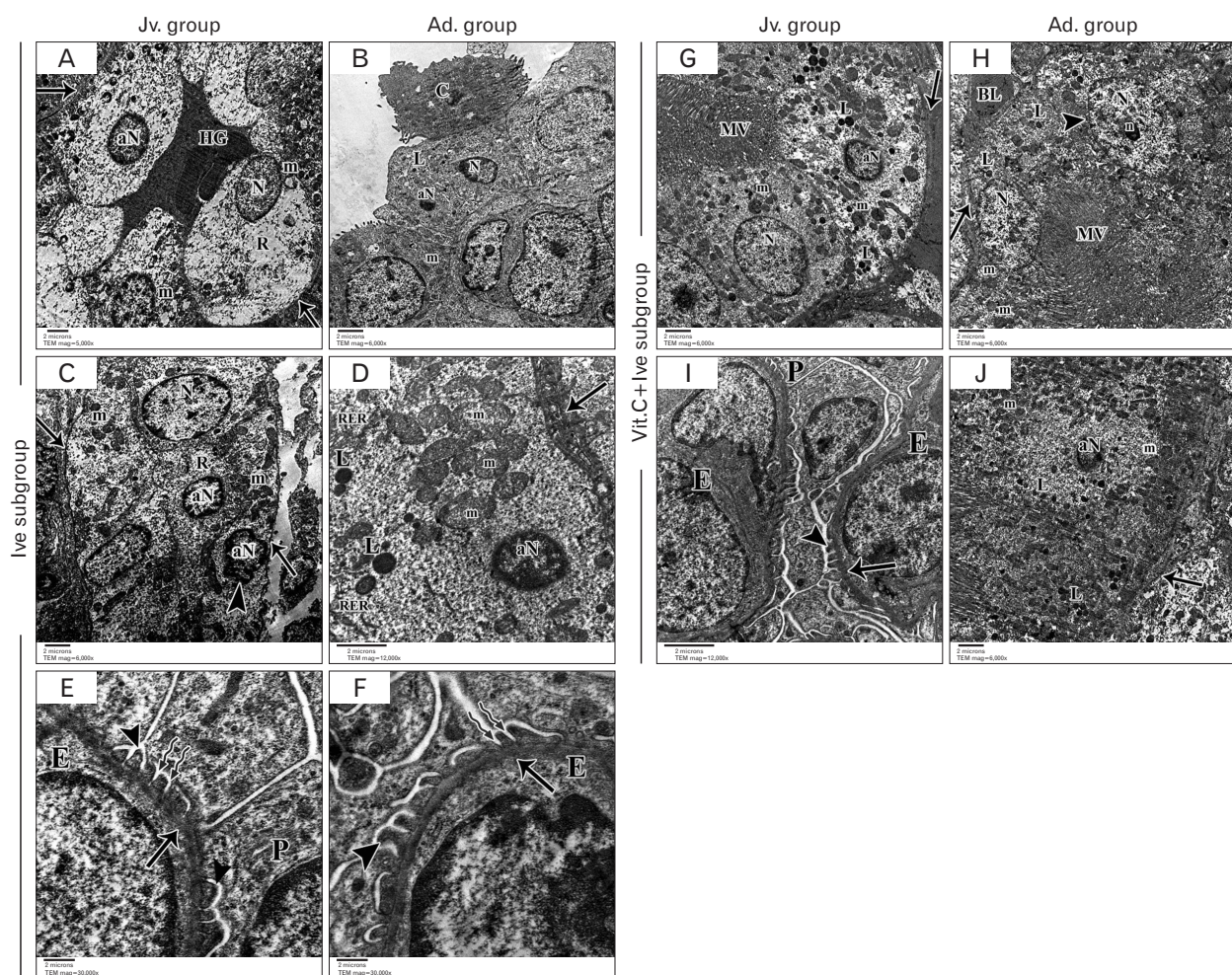


Fig. 7. Electron micrographs of kidney tubules of ivermectin (Ive) treated sub groups; juvenile (Jv) (A: proximal tubule, $\times 5,000$; C: distal tubule, $\times 6,000$) and adult (Ad) (B: proximal tubule, $\times 6,000$; D: distal tubule, $\times 12,000$) showing the following features: N, normal nucleus; aN, apoptotic nucleus; m, ballooned mitochondrial; R, cytoplasmic rarefaction; C, intraluminal casts; L, secondary lysosomes; RER, degenerated rough endoplasmic reticulum; HG, luminal hemorrhage; arrowhead, irregular nuclear envelop; arrow, thick basement membrane. The region of glomerulus in both Jv (E: $\times 30,000$) and Ad (F: $\times 30,000$) of the same subgroup with the following features: P, podosyt; arrow, thick basement membrane; arrowhead, fused foot process of podocytes; zigzag arrow, fused septum between foot process; E, endothelial cells. Vit.C+Ive subgroups of Jv (G: $\times 6,000$; I: $\times 12,000$), and Ad (H: $\times 6,000$; J: $\times 6,000$) rats showing N, normal nucleus; n, nucleolus; aN, apoptotic nucleus m, mitochondria; MV, microvilli; BL, blood capillary; L, lysosomes; arrow, basement membrane; arrow head, regular nuclear envelop in (H) and relatively normal foot process in (I). Moreover, glomerulus in (I) showing P, intact podocyte and E, endothelial cells.

mix of normal cells and apoptotic cells with scattered lysosomes (Fig. 7G), and the region of glomerulus showed intact podocytes and relatively normal foot processes and thick basement membrane (Fig. 7I).

Discussion

Ivermectin has been used for several years to treat many infectious diseases in mammals. Ivermectin was identified in late 1970 and first approved for animal use in 1981. Its potential use in humans was confirmed a few years later. Subsequently, Crump and Ōmura [39] who discovered and developed ivermectin owned the 2015 Nobel Prize [40]. Previous studies proved that ivermectin is a broad-spectrum drug [39, 40], having antiparasitic, antiviral, immunomodulation, cancer cells suppression and glucose and cholesterol regulation effects [8], consequently, it may play an essential role in the treatment of different types of viruses including COVID-19 [6], hope to help solving this pandemic disaster COVID-19 and because that adverse effects of ivermectin not yet investigated especially in juvenile age, this work was done to assess the toxic effect of ivermectin on renal structure and function in both juvenile and adult rats as recently it has consumed in high doses as a potent drug for treatment of cases of SARS-CoV-2 in both children and adult and also study the possible potential protective role of vitamin C since it was reported as the main additive drug used.

Effect of ivermectin investigated biochemically and the results showed an elevation in serum kidney function markers as presented in Table 2, the serum level of urea and creatinine increased upon treatment with ivermectin in comparison with the control group in both adult and juvenile rats. Comparing of both Ive subgroups, the juvenile group showed more elevated kidney function marker. Furthermore, consumption of vitamin C parallel with ivermectin in juvenile rats led to partial protection from this deterioration, while in adult rats vitamin C led to nearly full protection. These findings also highlighted the synergistic effect of oral antioxidant vitamin C on improving metabolism and renal function. These results were in line with [41] where the rabbits treated with ivermectin plus vitamin C showed a significant decrease in serum urea, supporting the action of vitamin C as a scavenger of free radicals. Also, Arise and Malomo [42] reported that ivermectin treated rats for 15 days developed a significant increase in urea and creatinine compared with the untreated group, thereby confirming reduced renal glo-

merular filtration.

Homogenate tissue analysis was done trying to understand the way by which ivermectin affect renal function, the TAC and activities of the antioxidant enzymes CAT, SOD, and GPx showed that rats treated with ivermectin (Ive subgroups) displayed a highly significant decrease TAC, CAT, SOD, and GPx with significant increase in ROS. While consumption of vitamin C parallel with ivermectin in both Vit. C+Ive subgroups exhibited stability of oxidant/antioxidant activities near control group. These results suggest that ivermectin causes damage in the kidney tissue due to production of an oxidative stress and that it's why the anti-oxidative activities of vitamin C could prevent these pathological and biochemical damage to kidney. Comparing juvenile and adult groups showed that juvenile rats had more decline in oxidants activity in treated group and less protected effect of vitamin C this was in accordance with Atakisi et al. [11], who revealed a decrease in the TAC in animal group that was treated with ivermectin. Carr and Maggini [43] reported that Impaired immunity and higher susceptibility to infections are outcomes of vitamin C deficiency. In turn, infections significantly impact on vitamin C levels due to enhanced inflammation and metabolic requirements. Furthermore, supplementation with vitamin C appears to be able to both prevent and treat respiratory and systemic infections. Moreover, vitamin C supplementation to *Gulo*^{-/-} mice, lacking the enzyme gulonolactone oxidase (*Gulo*) required for the biosynthesis of it, improves their metabolic profile and endoplasmic reticulum stress response and raises their life span [44].

In pathological conditions, over expression of MMP9 causes damage to epithelial lining leading to loss of cellular matrix and cytoskeleton damage [45], MMP9 mediate acute kidney injury due to different agents in glomeruli and tubular epithelial cells [46]. Furthermore, previous studies [47, 48] stated that induction of MMP9 promoted cytoskeleton disruption and loss of cell-cell adhesion. In this study, PCR examination had convincingly showed that MMP9 was statistically significantly higher in Ive subgroups compared to control which indicate basement membrane degradation. While consumption of Vit. C parallel with ivermectin exhibited partial stability against this degradation. Comparing juvenile and adult groups showed that adult rats had higher level of MMP9 in all subgroups. This was in accordance with Khan et al. [47], who stated that nephrotoxicity is correlated strongly with induction of MMP9 mRNA and protein in a

dose dependent manner. Further, while induction of MMP9 promoted cytoskeleton disruption and loss of cell–cell adhesion, inhibition of MMP9 was found to reduce these disruptions.

Further histological and morphometric examination of renal tissue confirmed the results obtained for the effect of ivermectin on serological and biochemical parameters in both juvenile and adult rats. Kidney sections revealed extremely shrunken glomeruli and a widened urinary space in between, proximal and distal convoluted tubules are dilated and their lining cells showed pyknotic nuclei with extensive cytoplasmic vacuolation, and epithelial cell exfoliations were also present, moreover, there were extensive extravasated blood and mononuclear cell infiltration. PAS-stained sections of Ive subgroups revealed strong positive PAS reaction of thickened basement membrane of both Bowman's capsule and renal tubules and discontinuity at the brush borders of proximal tubular cells, beside that there were ultra-structural alterations in which tubular cells displayed wide areas of cytoplasmic rarefaction, extremely degenerated irregular nuclei, mitochondria appeared ballooned with damaged cristae, markedly thickened irregular basal cell membrane and completely degenerated microvilli with extravasated blood in the lumen. The administration of vitamin C ameliorated the impact of the drug on the renal tissue. That was more obvious in adult rats as the pathological alteration in adult rats were less than the juvenile ones this was in agreement with Al Drees et al. [49], who studied the effect of ivermectin on multiple organs such as kidney, liver and testis and the role of vitamin C in correction of these alterations however they stated that combination of the use supplemented vitamins A and C showed promising results than vitamin C alone in ameliorating this toxic effects of ivermectin.

Immunohistochemically, significant increase of Bax expression (a proapoptotic protein) in our study especially in Ive subgroup in juvenile rats where the toxicity and renal damage were more abundant than adult group and that was corrected partially in juvenile and was nearer to normal in adult group after administration of vitamin C. This was in agreement with other studies that found the same result in rats experiencing other pathological conditions such as hemorrhagic shock [49]. Tait and Green [50] demonstrated that apoptosis is completely dependent on Bax/Bak at the level of the mitochondria because the lack of genes encoding these two proteins results in cells that resist apoptosis by preventing release of cytochrome c. However, other studies have

shown an indirect role of Bax/Bak in apoptosis and necrosis through release of cytochrome c and activation of caspases 3 and 8 [51]. In addition, Bax is responsible for the formation of these permeability pores leading to cell necrosis [52]. Therefore, the increased expression and activation of Bax as a result of ivermectin toxicity in both juvenile and adult rats may induce cell apoptosis.

In conclusion, administration of ivermectin led to attenuation in kidney function, decrease in the activities of the antioxidant enzymes and increase in MMP9 activity, significant histological and ultrastructural changes and increase in percentage of Bax proapoptotic protein expression. All these changes were more obvious in juvenile group while co-administration of vitamin C led to significant protection which was more in adult group. So, ivermectin should be used cautiously especially in juvenile age, and co-administration of vitamin C is highly recommended.

ORCID

Shereen E. Tawfeek:

<https://orcid.org/0000-0002-1372-6594>

Ayat M. Domouky:

<https://orcid.org/0000-0001-7516-629X>

Reham H. Abdel-Kareem:

<https://orcid.org/0000-0001-8285-4496>

Author Contributions

Conceptualization: SET. Data acquisition: RHAK. Data analysis or interpretation: AMD. Drafting of the manuscript: SET. Critical revision of the manuscript: RHAK. Approval of the final version of the manuscript: all authors.

Conflicts of Interest

No potential conflict of interest relevant to this article was reported.

Acknowledgements

Special thanks to Human Anatomy Department, Faculty of Medicine, Zagazig University. Many thanks to Zagazig University Animal House Department and Scientific Medical Research Center.

References

- Jiang F, Deng L, Zhang L, Cai Y, Cheung CW, Xia Z. Review of the clinical characteristics of coronavirus disease 2019 (COVID-19). *J Gen Intern Med* 2020;35:1545-9.
- Lu H, Stratton CW, Tang YW. Outbreak of pneumonia of unknown etiology in Wuhan, China: the mystery and the miracle. *J Med Virol* 2020;92:401-2.
- Sohrabi C, Alsafi Z, O'Neill N, Khan M, Kerwan A, Al-Jabir A, Iosifidis C, Agha R. World Health Organization declares global emergency: a review of the 2019 novel coronavirus (COVID-19). *Int J Surg* 2020;76:71-6.
- Reviglio VE, Osaba M, Reviglio V, Chiaradia P, Kuo IC, O'Brien TP. COVID-19 and Ophthalmology: a new chapter in an old story. *Med Hypothesis Discov Innov Ophthalmol* 2020;9:71-3.
- Caly L, Druce JD, Catton MG, Jans DA, Wagstaff KM. The FDA-approved drug ivermectin inhibits the replication of SARS-CoV-2 *in vitro*. *Antiviral Res* 2020;178:104787.
- Heidary F, Gharebaghi R. Ivermectin: a systematic review from antiviral effects to COVID-19 complementary regimen. *J Antibiot (Tokyo)* 2020;73:593-602.
- Omura S, Crump A. Ivermectin: panacea for resource-poor communities? *Trends Parasitol* 2014;30:445-55.
- Laing R, Gillan V, Devaney E. Ivermectin - old drug, new tricks? *Trends Parasitol* 2017;33:463-72.
- Yang SNY, Atkinson SC, Wang C, Lee A, Bogoyevitch MA, Borg NA, Jans DA. The broad spectrum antiviral ivermectin targets the host nuclear transport importin $\alpha/\beta 1$ heterodimer. *Antiviral Res* 2020;177:104760.
- Shoumann WM, Hegazy AA, Nafae RM, Ragab MI, Samra SR, Ibrahim DA, AL-Mahrouky TH, Sileem AE. Use of ivermectin as a potential chemoprophylaxis for COVID-19 in Egypt: a randomized clinical trial. *J Clin Diagn Res* 2021;15:OC27-32.
- Atakisi E, Atakisi O, Topcu B, Uzun M. Effects of therapeutic dose of ivermectin on plasma nitric oxide and total antioxidant capacity in rabbits. *Eur Rev Med Pharmacol Sci* 2009;13:425-9.
- Saha D. Role of free radicals, oxidative stress and xenobiotics in carcinogenesis by environmental pollutants. *Av Biomed* 2014;3:84-92.
- Nwani CD, Odo GE, Nwadinigwe AO, Onyeye CC, Atama CI, Ngwu G, Oluah SN, Ukonze JA, Ezeibe BC. Short-term effects of Albendazole on the oxidative stress markers and hematological parameters in tissues of African Catfish *Clarias gariepinus*. *J Aquat Anim Health* 2016;28:222-8.
- Budge PJ, Herbert C, Andersen BJ, Weil GJ. Adverse events following single dose treatment of lymphatic filariasis: observations from a review of the literature. *PLoS Negl Trop Dis* 2018;12:e0006454.
- Burnham GM. Adverse reactions to ivermectin treatment for onchocerciasis. Results of a placebo-controlled, double-blind trial in Malawi. *Trans R Soc Trop Med Hyg* 1993;87:313-7.
- Lukiana T, Mandina M, Situakibanza NH, Mbula MM, Lepira BF, Odio WT, Kamgno J, Boussinesq M. A possible case of spontaneous *Loa loa* encephalopathy associated with a glomerulopathy. *Filaria J* 2006;5:6.
- Kaur U, Chakrabarti SS, Gambhir IS. Delirium induced by albendazole-ivermectin combination: report of the first case in an older patient. *Geriatr Gerontol Int* 2017;17:2618-20.
- Veit O, Beck B, Steuerwald M, Hatz C. First case of ivermectin-induced severe hepatitis. *Trans R Soc Trop Med Hyg* 2006;100:795-7.
- Choksi TT, Madison G, Dar T, Asif M, Fleming K, Clarke L, Danilewitz M, Hennawy R. Multiorgan dysfunction syndrome from strongyloides stercoralis hyperinfection in a patient with human T-cell lymphotropic virus-1 coinfection after initiation of ivermectin treatment. *Am J Trop Med Hyg* 2016;95:864-7.
- Almeida MG, Röpke CD, Davino SC, Nobre FAF, Santos E, Barros SBM. P1C84 - Modulation of hexachlorobenzene induced liver oxidative stress by α -Tocopherol. *Toxicol Lett* 1998;95(Suppl 1):57.
- Abubakar MG, Taylor A, Ferns GA. Regional accumulation of aluminium in the rat brain is affected by dietary vitamin E. *J Trace Elem Med Biol* 2004;18:53-9.
- Holford P, Carr AC, Jovic TH, Ali SR, Whitaker IS, Marik PE, Smith AD. Vitamin C-an adjunctive therapy for respiratory infection, sepsis and COVID-19. *Nutrients* 2020;12:3760.
- El-Demerdash FM, Yousef MI, Zoheir MA. Stannous chloride induces alterations in enzyme activities, lipid peroxidation and histopathology in male rabbit: antioxidant role of vitamin C. *Food Chem Toxicol* 2005;43:1743-52.
- Kojo S. Vitamin C: basic metabolism and its function as an index of oxidative stress. *Curr Med Chem* 2004;11:1041-64.
- Yavuz T, Delibas N, Yildirim B, Altuntas I, Candir O, Cora A, Karaman N, Ibrism E, Kutsal A. Vascular wall damage in rats induced by methidathion and ameliorating effect of vitamins E and C. *Arch Toxicol* 2004;78:655-9.
- Aversa R, Victoria R, Petrescu V, Apicella A, Petrescu F. We are addicted to vitamins C and E-A review. *Am J Eng Appl Sci* 2016;9:1003-18.
- Zuhair Z, AL-amri H. The role of vitamin C in alteration of enzymes responsible of energy metabolism induced by administration of tamoxifen to mouse. *Adv Biol Chem* 2011;1:15-23.
- Arise RO, Malomo SO, Oyewole OI. Histological changes in selected tissues of ivermectin and/or albendazole treated rats. *Int J Toxicol Appl Pharmacol* 2012;2:1-5.
- Khan RA, Khan MR, Sahreen S. Brain antioxidant markers, cognitive performance and acetylcholinesterase activity of rats: efficiency of *Sonchus asper*. *Behav Brain Funct* 2012;8:21.
- Ebrahimi Z, Khazaei MR, Ghanbari E, Khazaei M. Renal tissue damages and its antioxidant status improved by crab shell extract in streptozotocin-induced diabetic rat. *Adv Biomed Res* 2019;8:41.
- Maehly AC, Chance B. The assay of catalases and peroxidases. *Methods Biochem Anal* 1954;1:357-424.
- Kakkar P, Das B, Viswanathan PN. A modified spectrophotometric assay of superoxide dismutase. *Indian J Biochem Biophys* 1984;21:130-2.
- Mohandas J, Marshall JJ, Duggin GG, Horvath JS, Tiller DJ.

- Differential distribution of glutathione and glutathione-related enzymes in rabbit kidney. Possible implications in analgesic nephropathy. *Biochem Pharmacol* 1984;33:1801-7.
34. Bengatta S, Arnould C, Letavernier E, Monge M, de Préneuf HM, Werb Z, Ronco P, Lelongt B. MMP9 and SCF protect from apoptosis in acute kidney injury. *J Am Soc Nephrol* 2009;20:787-97.
 35. Schmittgen TD, Livak KJ. Analyzing real-time PCR data by the comparative C(T) method. *Nat Protoc* 2008;3:1101-8.
 36. Cakici O, Akat E. Effects of oral exposure to diazepam on mice liver and kidney tissues: biometric analyses of histopathologic changes. *Anal Quant Cytopathol Histopathol* 2013;35:7-16.
 37. Cui JH, Qiao Q, Guo Y, Zhang YQ, Cheng H, He FR, Zhang J. Increased apoptosis and expression of FasL, Bax and caspase-3 in human lupus nephritis class II and IV. *J Nephrol* 2012;25:255-61.
 38. Glauert AM, Lewis PR. Other embedding media. In: Glauert AM, Lewis PR, editors. *Biological Specimen Preparation for Transmission Electron Microscopy*. Princeton: Princeton University Press; 2014. p.279-92.
 39. Crump A, Ōmura S. Ivermectin, 'wonder drug' from Japan: the human use perspective. *Proc Jpn Acad Ser B Phys Biol Sci* 2011;87:13-28.
 40. González Canga A, Sahagún Prieto AM, Díez Liébana MJ, Fernández Martínez N, Sierra Vega M, García Vieitez JJ. The pharmacokinetics and interactions of ivermectin in humans--a mini-review. *AAPS J* 2008;10:42-6.
 41. Al-Jassim KB, Jawad AAH, Al-Masoudi EA, Majeed SK. Histopathological and biochemical effects of ivermectin on kidney functions, lung and the ameliorative effects of vitamin C in rabbits (*Lupus cuniculus*). *Basrah J Vet Res* 2016;15:110-24.
 42. Arise RO, Malomo SO. Effects of ivermectin and albendazole on some liver and kidney function indices in rats. *Afr J Biochem Res* 2009;3:190-7.
 43. Carr AC, Maggini S. Vitamin C and immune function. *Nutrients* 2017;9:1211.
 44. Aumailley L, Warren A, Garand C, Dubois MJ, Paquet ER, Le Couteur DG, Marette A, Cogger VC, Lebel M. Vitamin C modulates the metabolic and cytokine profiles, alleviates hepatic endoplasmic reticulum stress, and increases the life span of *Gulo*^{-/-} mice. *Aging (Albany NY)* 2016;8:458-83.
 45. LeBert DC, Squirrel JM, Rindy J, Broadbridge E, Lui Y, Zakrzewska A, Eliceiri KW, Meijer AH, Huttenlocher A. Matrix metalloproteinase 9 modulates collagen matrices and wound repair. *Development* 2015;142:2136-46.
 46. Catania JM, Chen G, Parrish AR. Role of matrix metalloproteinases in renal pathophysiology. *Am J Physiol Renal Physiol* 2007;292:F905-11.
 47. Khan H, Singh RD, Tiwari R, Gangopadhyay S, Roy SK, Singh D, Srivastava V. Mercury exposure induces cytoskeleton disruption and loss of renal function through epigenetic modulation of MMP9 expression. *Toxicology* 2017;386:28-39.
 48. Tsur A, Bening Abu-Shach U, Broday L. ULP-2 SUMO protease regulates E-cadherin recruitment to Adherens junctions. *Dev Cell* 2015;35:63-77.
 49. Al Drees A, Salah Khalil M, Soliman M. Histological and immunohistochemical basis of the effect of aminoguanidine on renal changes associated with hemorrhagic shock in a rat model. *Acta Histochem Cytochem* 2017;50:11-9.
 50. Tait SW, Green DR. Mitochondria and cell death: outer membrane permeabilization and beyond. *Nat Rev Mol Cell Biol* 2010;11:621-32.
 51. Whelan RS, Konstantinidis K, Wei AC, Chen Y, Reyna DE, Jha S, Yang Y, Calvert JW, Lindsten T, Thompson CB, Crow MT, Gavathiotis E, Dorn GW 2nd, O'Rourke B, Kitsis RN. Bax regulates primary necrosis through mitochondrial dynamics. *Proc Natl Acad Sci U S A* 2012;109:6566-71.
 52. Karch J, Kwong JQ, Burr AR, Sargent MA, Elrod JW, Peixoto PM, Martinez-Caballero S, Osinska H, Cheng EH, Robbins J, Kinnally KW, Molkentin JD. Bax and Bak function as the outer membrane component of the mitochondrial permeability pore in regulating necrotic cell death in mice. *Elife* 2013;2:e00772.